

Synthesis of the Novel MAX Phases for the Future Nuclear Fuel Cladding and Structural Materials

Seung Hyeok Chung^a, Taehee Kim^b, Taegy Lee^b, H. J. Ryu^{b*}

^aKyunghee Univ., Nuclear Engineering Dept. 1732, Deogyong-daero, Giheung-gu, Yongin-si, Gyeonggi-do, Republic of Korea

^bKorea Advanced Institute of Science and Technology, Nuclear & Quantum Engineering Dept. 291 Daehakro, Yuseong, 34141, Republic of Korea

*Corresponding author: hojinryu@kaist.ac.kr

1. Introduction

The MAX phases are the ternary compounds which have general chemical formula $M_{n+1}AX_n$, where $n=1$ to 3, M is an early transitional metal, A is an element in group 13 to 16, and X is C and/or N [1]. M has metallic bonding with A and covalent bonding with X. Elements are marked in the periodic table in Fig. 1, where M elements are marked in red, A in blue, and X in black.

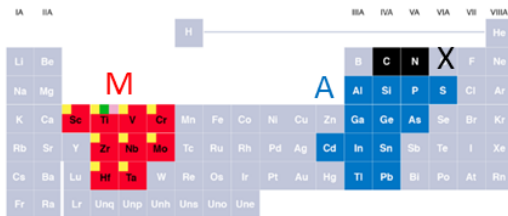


Fig. 1. Periodic table illustrating elements forming the MAX phase.

Because of its laminated crystal structure which has M_6X octahedral interleaved with A-layers and the presence of active basal slip, these ternary compounds possess exceptional properties such as superb machinability, good thermal and electrical conductor, damage tolerance and very resistant to thermal shock like metal. Furthermore, the MAX phase possesses the properties such as oxidation and corrosion resistant in extreme condition, refractory, low density, high stiffness and low thermal expansion like ceramics [2]

With these properties, the MAX phases are expected to be used for the Accident Tolerant Fuel (ATF) cladding and oxidation/corrosion resistance materials. Especially, the MAX phase can be used for the Gen-IV, SFR and HTGR, component materials which have to possess the thermal and corrosion resistance.

The zirconium has been used to the nuclear industry for fuel cladding because of the small thermal neutron cross-section. Zr-based MAX phase was discovered by group Lapauw et al. [3,4]. They observed the Zr_2AlC and Zr_3AlC_2 with the X-ray diffraction (XRD) patterns and backscattered electron detector.

Some solid solutions allow for the formation of the MAX phase of certain M element [5]. There are two scenarios for the formation of MAX phases: (1) the nucleation scenario i.e. reaction between M-A based intermetallic and MX material followed by nucleation

and growth of Max phases and, (2) The intercalation scenario, i.e. A material intercalation into MX material and subsequent MAX phase formation [6]. There are so many attempts to add the elements in the Zr-based MAX phase due to the properties of zirconium for the nuclear applications. The solid solubility of Zr in the Nb_4AlC_3 was investigated by Lapauw et al. The $(Nb_x, Zr_{1-x})_4AlC_3$ crystal structure was investigated by the XRD and NPD. The $(Nb_{0.85}, Zr_{0.15})_4AlC_3$ MAX phases were prepared from a powder mixture with NbH_2 , ZrH_2 , Al, C by reactive hot pressing at $1700^\circ C$ for 30 minutes. The maximal solubility of Zr was 18.5% of Nb content in the Nb_4AlC_3 [7].

Above this, other compounds have been attempted. The $(Ti_{0.5}, V_{0.5})_2AlC$, $(Ti_{0.5}, Nb_{0.5})_4AlC_3$ and $(Ti_{0.5}, Nb_{0.5})_3AlC_2$ MAX phase were discovered and observed by Anasori et al., using Rietveld analysis of the XRD patterns. These MAX phases were prepared from a powder mixture with Ti, V, Nb, Al, C by argon tube furnace at $1450^\circ C$ for 2 hours [8].

In this study, the multi-component MAX phase based on the reference MAX phases, the $(Nb_x, Zr_{1-x})_4AlC_3$ and $(Ti_{0.5}, V_{0.5})_2AlC$, was investigated. The Spark Plasma Sintering (SPS) was selected for production method. Furthermore, sintered materials were analyzed by the scanning electron microscope (SEM), the X-ray diffraction (XRD), Energy Dispersive Spectrometry (EDS). The cross-section and the top surface were used to obtain the EDS/SEM and XRD respectively.

2. Experimental details

To applicate the MAX phase for future nuclear fuel cladding materials, Zr has been studied for the element for M site because of its small thermal neutron cross-section [9]. Ti, Nb, Cr are used for alloying elements in commercial fuel cladding such as Zircaloy, ZIRLO or 15-15 Ti-SS [10,11]. V has good corrosion resistance, a small neutron cross-section and it is not brittle. Moreover, V is harder than most metals and steels. Al forms a protective oxide scale (Al_2O_3) that does not spall off during thermal cycling. C is used instead of N for this study to prevent the formation of the long-lived isotope ^{14}C caused by irradiation of N. The experiment cases for this study are summarized in Table I.

Table I: The experiment cases for this study.

No.	Targeted compound
1	$(\text{Nb}_{0.5}\text{Zr}_{0.5})_4\text{AlC}_3$
2	$(\text{Zr}_{0.5}\text{Cr}_{0.5})_4\text{AlC}_3$
3	$(\text{Nb}_{0.5}\text{Cr}_{0.5})_4\text{AlC}_3$
4	$(\text{V}_{0.5}\text{Ti}_{0.5})_2\text{AlC}$
5	$(\text{Nb}_{0.5}\text{Cr}_{0.5})_4\text{AlC}_3$

The starting powders that used in this study were synthesized from ZrH_2 (>99%, -325 mesh, Alfa Aesar), Nb (>99.8%, -60 mesh, Aldrich), Cr (>99.5%, -100 mesh, Aldrich), V (>99.5%, -100 mesh, Aldrich), Ti (>99.7%, -100 mesh, Aldrich), Al (>99.8%, -40+325 mesh, Alfa Aesar), C (>99%, <20 μm , Aldrich). The powders were mixed in a stoichiometric ratio of 4 : 1.5 : 2.8 for n=3 and 2 : 1.5 : 0.8 for n=1. This is in order to compensate the usual sublimation of Aluminum and invasion of carbon from graphite mold. Powders were mixed in a plastic jar using a 3-D tubular mixer with ZrO_2 balls ($\Phi=3$ mm, 100 rpm for 3 h) to make particles size finely. After mixing, the powder mixture was filled to the graphite mold ($\Phi=20$ mm) that was coated with B-N liquid. The Graphite mold with the powder mixture was placed in the Spark Plasma Sintering (SPS) furnace in vacuum mode and heated to the desired temperature on the graphite mold and pressured to the desired pressure on the top and bottom sides of the mold. Three different synthesis temperature and two different pressure and sintering time were used. The heating rate was set at 100°C/min for all seven cases of the experiment. Desired temperature and pressure for each experiment cases are summarized specifically in Table II.

Table II: Targeted compounds and conditions for using SPS.

No.	Temperature [°C]	Pressure [MPa]	Time [min]
1	1700	50	3
2	1500	50	5
3	1500	50	3
4	1300	50	3
5	1500	35	3

The element compositions of sintered materials are determined by the XRD (D/MAX-2500, RIGAKU). The top surface of the disc sample was used to obtain XRD patterns. The microstructure was observed by the SEM (SU8230, HITACHI) with the energy dispersive spectrometer (EDS). The entire experiment procedure is summarized in Fig. 2.

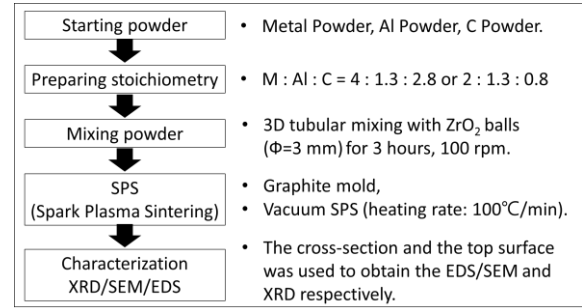


Fig. 2. Schematic of experiment procedure

3. Results and discussion

Table III: Targeted compounds and predicted crystalline phases by XRD/EDS

No.	Predicted crystalline phases
1	NbC, ZrC, ZrAl_2 , Zr_2Al_3
2	ZrC, ZrAl_2 , Zr_2Al_3 , Zr₄AlC₃ , Zr₂AlC , Zr₃AlC₂
3	NbC, NbAl ₂ , CrC
4	VC, TiC, Ti_2Al_3 , VAl ₃
5	NbC, NbAl ₂ , CrC

The outputs of synthesized material are summarized in Table III. The results of synthesis are predicted by the XRD patterns and EDS data. Most XRD and EDS data are described that the MAX phases were not obtained except experiment number 2. Most cases of experiment sintered samples have carbide and metal alloys. Experiment number 2 has Zr, Al and C in the partial region SEM images are presented in Fig. 3. Left image of Fig. 3 is across-section image of $(\text{Zr}_{0.5}\text{Cr}_{0.5})_4\text{AlC}_3$ targeting material. Formed crystalline phases partially have different elements composition. We can expect that the red circles (EDS spot 3, 4, 6), which are located in the dark region, on the right image of Fig. 3 have the possibility of the MAX phase formation according to the EDS data in Fig. 4., while the blue circles (EDS spot 1, 2, 5) which are located in the light regions on the right image of Fig. 3 might be formed ZrC or Zr-alloy.

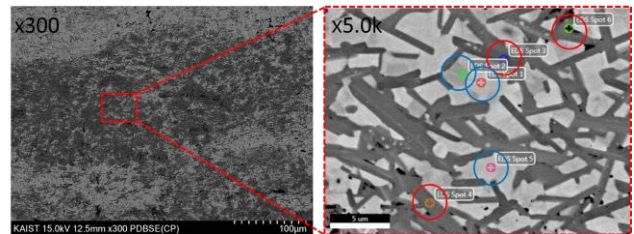


Fig. 3. SEM image of $(\text{Zr}_{0.5}\text{Cr}_{0.5})_4\text{AlC}_3$ targeting material

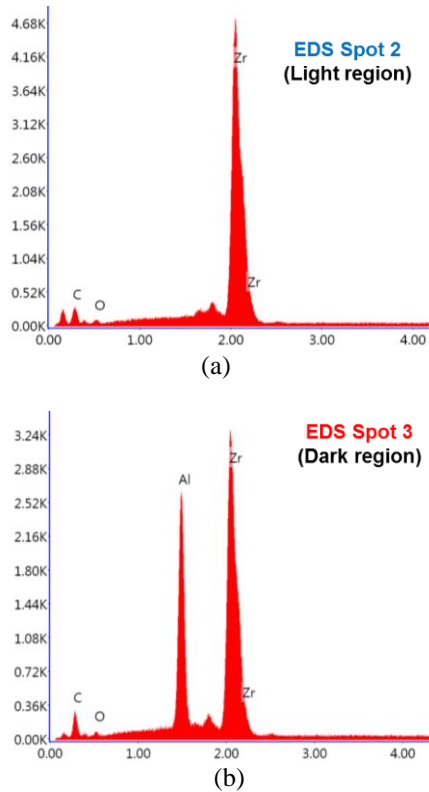


Fig. 4 EDS pointing analysis data of $(Zr_{0.5}Cr_{0.5})_4AlC_3$ targeting material, experiment number 2, (a) EDS spot 2 (Light region), (b) EDS spot 3 (Dark region).

Zr_3AlC_2 is formed in $(Zr_{0.5}Cr_{0.5})_4AlC_3$ targeting material according to the XRD patterns in Fig. 5. The XRD patterns of $(Zr_{0.5}Cr_{0.5})_4AlC_3$ targeting material have a good agreement with the XRD patterns of Zr_3AlC_2 [4]. Therefore, the dark region of $(Zr_{0.5}Cr_{0.5})_4AlC_3$ targeting material has a MAX phase of Zr_3AlC_2 .

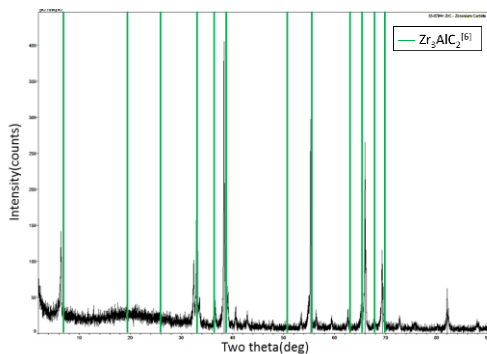


Fig. 5 XRD patterns of $(Zr_{0.5}Cr_{0.5})_4AlC_3$ targeting material

4. Conclusions

Fabrication of the Zr-containing MAX phase was investigated for nuclear fuel cladding and structural materials applications. A MAX phase with the Zr_3AlC_2 structure was synthesized by spark plasma sintering of a powder mixture targeting $(Zr_{0.5}Cr_{0.5})_4AlC_3$. The formation of MAX phases was confirmed by XRD and

EDS of sintered samples. In the future work, the electron probe micro analyzer (EPMA) and transmission electron microscopy (TEM) are required to certain analyze the elements composition and formation of the MAX phase.

Acknowledgments

This study was supported by the KUSTAR-KAIST Institute.

REFERENCES

- [1] MAX/MXene Research Group Homepage of Department of Material Science and Engineering, Drexel University. (2016). <http://max.materials.drexel.edu/research-areas/max-phases/>
- [2] Radovic, M., & Barsoum, M. W. (2013). MAX phases: bridging the gap between metals and ceramics. *American Ceramics Society Bulletin*, 92(3), 20-27.
- [3] Lapauw, T., Lambrinou, K., Cabioc'h, T., Halim, J., Lu, J., Pesach, Rivin. O, Ozeri. O, Caspi. E.N., Hultman. L, Eklund. P, Rosen. J, Barsoum. M.W, Vleugels. J, (2016). Synthesis of the new MAX phase Zr_2AlC . *Journal of the European Ceramic Society*, 36(8), 1847-1853.
- [4] Lapauw, T, Halim, J, Lu, J, Cabioc'h, T, Hultman, L, Barsoum, M. W, Lambrinou, K, Vleugels, J, (2016). Synthesis of the novel Zr_3AlC_2 MAX phase. *Journal of the European Ceramic Society*, 36(3), 943-947.
- [5] Horlait, D., Grasso, S., Chroneos, A., & Lee, W. E. (2016). Attempts to synthesise quaternary MAX phases (Zr, M) $_2AlC$ and $Zr_2(Al, A)C$ as a way to approach Zr_2AlC . *Materials Research Letters*, 1-8.
- [6] Springer, H., & Raabe, D. (2012). Rapid alloy prototyping: Compositional and thermo-mechanical high throughput bulk combinatorial design of structural materials based on the example of 30Mn-1.2 C-xAl triplex steels. *Acta Materialia*, 60(12), 4950-4959.
- [7] Lapauw, T., Tytko, D., Vanmeensel, K., Huang, S., Choi, P. P., Raabe, D., ... & Lambrinou, K. (2016). $(Nb_x, Zr_{1-x})_4AlC_3$ MAX Phase Solid Solutions: Processing
- [8] Anasori, B., Dahlqvist, M., Halim, J., Moon, E. J., Lu, J., Hosler, B. C., ... & Rosén, J. (2015). Experimental and theoretical characterization of ordered MAX phases Mo_2TiAlC_2 and $Mo_2Ti_2AlC_3$. *Journal of Applied Physics*, 118(9), 094304.
- [9] Lambrinou, K., Lapauw, T. and Vleugels, J. (2015). Exploring the Potential of MAX Phases for Select Applications in Extreme Environments.
- [10] Delville, R., Stergar, E., & Verwerft, M. (2014, July). Results of a New Production of Nuclear-Grade 1.4970 '15-15Ti' Stainless Steel Fuel Cladding Tubes for GEN IV Reactors. In 2014 22nd International Conference on Nuclear Engineering (pp. V001T02A015-V001T02A015). American Society of Mechanical Engineers.
- [11] Rafique, M., Afzal, N., Ahmad, R., Ahmad, S., & Ghauri, I. M. (2012). Mechanical behavior of low-dose neutron-irradiated polycrystalline zirconium. *Radiation Effects and Defects in Solids*, 167(4), 289-297.